A MODEL OF PERITUBULAR CAPILLARY CONTROL OF ISOTONIC FLUID REABSORPTION BY THE RENAL PROXIMAL TUBULE

W. M. DEEN, C. R. ROBERTSON, *and* B. M. BRENNER

From the Department of Chemical Engineering, Stanford University, Stanford, California 94305, the Department of Medicine, Veterans Administration Hospital, San Francisco, California 94121, and the Department of Medicine, University of California, San Francisco, California 94122

ABSTRACT A mathematical model of peritubular transcapillary fluid exchange has been developed to investigate the role of the peritubular environment in the regulation of net isotonic fluid transport across the mammalian renal proximal tubule. The model, derived from conservation of mass and the Starling transcapillary driving forces, has been used to examine the quantitative effects on proximal reabsorption of changes in efferent arteriolar protein concentration and plasma flow rate. Under normal physiological conditions, relatively small perturbations in protein concentration are predicted to influence reabsorption more than even large variations in plasma flow, a prediction in close accord with recent experimental observations in the rat and dog. Changes either in protein concentration or plasma flow have their most pronounced effects when the opposing transcapillary hydrostatic and osmotic pressure differences are closest to equilibrium. Comparison of these theoretical results with variations in reabsorption observed in micropuncture studies makes it possible to place upper and lower bounds on the difference between interstitial oncotic and hydrostatic pressures in the renal cortex of the rat.

INTRODUCTION

In the peripheral microcirculation, the changing profile of pressures, which favor net ultrafiltration at the arterial end of the capillary and reabsorption at the venous end, derives primarily from a progressive decline in the transcapillary hydrostatic pressure difference (ΔP) from a level slightly greater than, to a level slightly less than, the opposing colloid osmotic pressure difference ($\Delta\pi$) (1–6). In the mammalian kidney, an organ characterized by extremely high rates of transcapillary fluid movement, not only are the sites for ultrafiltration and reabsorption anatomically distinct, but the profiles of transcapillary pressures governing fluid movement at these separate sites appear to differ markedly from profiles in the peripheral microcirculation.

As shown for the rat in Fig. 1, ΔP is relatively constant with distance along the

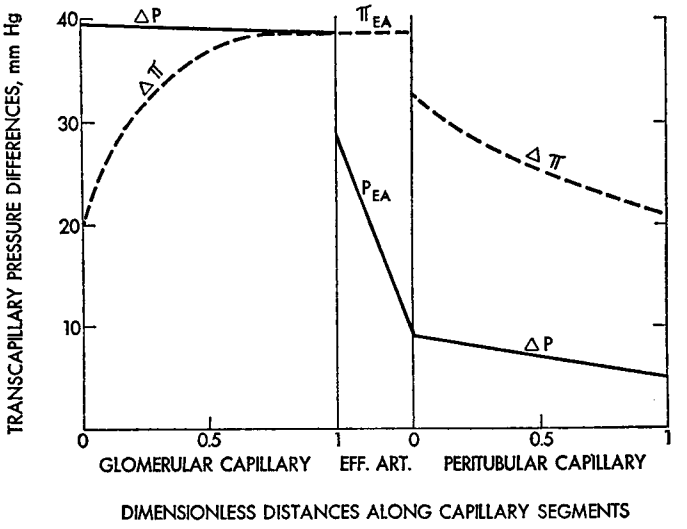

FIGURE 1 Approximate transcapillary pressure profiles in the rat kidney.

glomerular capillary, while the net driving force for ultrafiltration, $\Delta P - \Delta\pi$, diminishes primarily as a consequence of the increase in $\Delta\pi$ resulting from the formation of an essentially protein-free ultrafiltrate (7–9). The close equality of opposing hydrostatic and osmotic forces normally achieved before the end of the glomerulus has been termed "filtration pressure equilibrium."

As a result of the hydrostatic pressure drop along the efferent arteriole, the net driving pressure in the peritubular capillaries favors reabsorption. This driving pressure exceeds that found in peripheral capillaries as a consequence of the high oncotic pressure of postglomerular plasma and the relatively low peritubular capillary hydrostatic pressure (7–12).

In the steady state, assuming lymph production to be negligible, the rate of uptake of isotonic reabsorbate by the peritubular capillaries must be equal to the rate of tubular reabsorption. The rate of reabsorption by the proximal tubule may then be related to the mean transcapillary driving force according to

$$\text{APR} = K_r \bar{P}_r, \tag{1}$$

where APR is the volume reabsorbed per unit time (absolute proximal reabsorption), $\bar{P}_r$ is the mean transcapillary driving pressure, and K_r is a coefficient which is the product of the effective hydraulic permeability[1] and the surface area available

[1] The effective hydraulic permeability (k), measured in the presence of an osmotically active solute, will in general differ from the hydraulic permeability measured using pure water (L_p). k is defined by using the radially averaged protein concentration to compute osmotic pressure, but the concentration at the capillary wall and thus the true osmotic pressure are likely to be somewhat different. Under these conditions, a radial concentration gradient will be manifested as a resistance to transcapillary fluid movement (R) in series with that presented by the capillary wall: $1/k = (1/L_p) + R$.

for reabsorption. The driving force at any point along a capillary is given by

$$P_r = \Delta\pi - \Delta P,$$

$$= (\pi_C - \pi_I) - (P_C - P_I), \quad (2)$$

where π_C and P_C are the intracapillary oncotic and hydrostatic pressures, respectively, and π_I and P_I are the corresponding pressures in the cortical interstitium. While not appearing explicitly in Eqs. 1 or 2, postglomerular plasma flow rate must modify the effective driving force by causing a given volume of reabsorbate to dilute plasma proteins (lowering π_C) the lower the flow rate, the more the dilution. Hence, changes in plasma flow would be expected to cause parallel changes in capillary uptake.

The major difficulty in the estimation of either $\bar{P}_r$ or P_r is that direct methods for measurement of P_I and π_I are lacking. This again contrasts with the case for the glomerulus where the "interstitial fluid" (tubule fluid), readily accessible in Bowman's space, permits the precise estimation of π_I and P_I. For the peritubular capillary pressure profiles shown in Fig. 1, we arbitrarily assumed $P_I = 0$ and $\pi_I =$ 6 mm Hg. Depending on the value of $\pi_I - P_I$, the actual transcapillary pressure differences may be closer to or farther from equilibrium than as shown.

The proximity of the final values of ΔP and $\Delta\pi$ has been shown in a recent analysis of glomerular ultrafiltration to determine the degree to which glomerular filtration rate (GFR) is plasma-flow dependent (13). In the rat glomerulus, where equilibrium is normally achieved, single nephron GFR has been observed to increase (8) or decrease (9) essentially in proportion to changes in initial glomerular plasma flow, in agreement with theoretical predictions (13). Therefore, it is logical to suppose that peritubular capillary uptake will show more or less flow dependence as a function of the value of $\pi_I - P_I$. While it is not yet possible to measure π_I and P_I directly, it has recently been possible to measure the extent to which APR is plasma-flow dependent in the rat (11, 12, 14, 15). Accordingly, these measurements, taken together with an appropriate model, should provide insight into the probable range of values for $\pi_I - P_I$ for this species.

In the present study a simple mathematical model of peritubular transcapillary fluid exchange has been developed to investigate the relative importance of postglomerular plasma flow and protein concentration in the control of net fluid reabsorption by the renal proximal tubule. The model has been used to interpret the results of a number of experimental studies dealing with the forces governing proximal reabsorption.

GLOSSARY OF SYMBOLS

a_1, a_2 Osmotic pressure coefficients in Eq. 9, mm Hg/(g/100 ml) and mm Hg/(g/100 ml)^2, respectively.

APR	Absolute proximal reabsorption, nl/min.
B_1 , B_2	Dimensionless osmotic pressure coefficients, Eqs. 7 and 8.
C	Plasma protein concentration, g/100 ml.
C^*	Dimensionless protein concentration, C/C_{EA} .
H	Permeability and plasma flow rate parameter, Eq. 4.
I_1 , I_2 , I_3 , I_4	Integration constants in Eqs. A 7, A 9, A 10, and A 11, respectively.
k	Membrane effective hydraulic permeability, nl/(min·mm Hg·cm²).
K_r	Reabsorption coefficient, nl/(min·mm Hg), Eq. 1.
L	Length of capillary, cm.
m	Mass flow rate of protein in capillary, g/min.
P	Hydrostatic pressure, mm Hg.
P_r	Local net transcapillary driving pressure, mm Hg, Eq. 2.
ΔP	$P_C - P_I$, transcapillary hydrostatic pressure difference, mm Hg.
ΔP_C	Axial pressure drop along capillary, mm Hg.
Q	Volumetric flow rate in capillary, nl/min.
S	Capillary surface area, cm².
T	Defined by Eq. A 8.
x	Distance along idealized capillary from point at which reabsorption begins, cm.
x^*	Dimensionless distance along capillary, x/L.
	Greek Letters
α	Interstitial pressure parameter, Eq. 5.
β	Dimensionless axial pressure drop, Eq. 6.
π	Colloid osmotic pressure, mm Hg.
$\Delta\pi$	$\pi_C - \pi_I$, transcapillary osmotic pressure difference, mm Hg.
	Superscripts
$-$	Mean value.
*	Dimensionless variable.
	Subscripts
C	Peritubular capillary.
EA	Efferent arteriole.
I	Cortical interstitium.

MODEL DEVELOPMENT

The part of the peritubular capillary network considered here is defined as that which exchanges fluid with proximal convoluted tubule segments present on the surface of the renal cortex. These tubule segments, accessible to micropuncture, comprise about two-thirds of the total length of the proximal tubule, and reabsorb some 50% of the total volume of filtrate produced by their glomeruli (11, 12). This definition enables the model to relate directly to estimates of APR up to the usual site of micropuncture in last accessible proximal convolutions.[2]

[2] APR, the absolute rate of fluid reabsorption to the site of puncture in last accessible proximal tubule segments, is calculated from the equation APR = SNGFR − V_{TF} , where SNGFR is the single nephron GFR and V_{TF} is the volume of tubule fluid collected per unit time at the site of puncture. SNGFR is determined experimentally from measurements of tubule fluid to plasma inulin concentration ratio, $(TF/P)_{In}$, and V_{TF} , according to the expression: SNGFR = $(TF/P)_{In} \cdot V_{TF}$.

The fundamental assumption made here is that peritubular capillary uptake, not transport across the tubule, is the step which limits net reabsorption. In support of this assumption are the findings, reviewed in detail elsewhere (12, 14), which indicate that APR is relatively insensitive to changes in tubule geometry, tubule fluid flow rate, and filtered load of sodium, but highly sensitive to perturbations in the peritubular environment such as changes in peritubular capillary protein concentration. Consistent with this assumption that peritubular capillary uptake of reabsorbate is rate limiting is the observation that the unidirectional flux of sodium out of the proximal tubule far exceeds the net flux (16–19), indicating that the tubules provide more reabsorbate than is actually taken up by the capillaries.

Proximal tubules are surrounded by a highly branched network of peritubular capillaries. For simplicity, this network will be treated as a single tube of equivalent total surface area, in which radial concentration gradients and the details of capillary hemodynamics have been neglected. Axial diffusion within the capillary will likewise be neglected. Since it is assumed that hydrostatic pressure or colloid concentration gradients do not exist within the interstitium (π_I and P_I constant), assumptions about the geometrical relationship of the idealized capillary to the corresponding tubule (i.e., cocurrent or countercurrent flow) are not required.

By choosing Eq. 2 to represent the local driving force for reabsorption, we assume that the capillary is completely impermeable to plasma proteins (reflection coefficients, $\sigma = 1$). While the value of σ for albumin is probably less than unity, its exact value remains uncertain. Moreover, setting $\sigma < 1$ for any solute requires knowledge of the corresponding solute mobility (20). Since experimental data sufficient to characterize the capillary membrane according to even a simple thermodynamic analysis are not yet available, the present approach is appropriate for a first approximation to the quantitative description of peritubular transcapillary fluid exchange. The test of these assumptions is the extent to which the model aids in the interpretation of the available data on reabsorption.

An equation which expresses the rate of change of protein concentration (C) with distance (x) along an idealized capillary, in the steady state, can be obtained from a simple mass balance (see Appendix). When distance ($0 \leq x^* \leq 1$) and concentration are nondimensionalized, this equation becomes

$$\frac{dC^*}{dx^*} = HC^{*2}\left[\alpha - \beta\left(x^* - \frac{1}{2}\right) - (B_1 C^* + B_2 C^{*2})\right], C^*(0) = 1, \quad (3)$$

where $C^* = C/C_{EA}$ and C_{EA} is the protein concentration in the efferent arteriole. The quantities H, α, β, B_1, and B_2 are dimensionless parameters defined as follows:

$$H = \frac{K_f \pi_{EA}}{Q_{EA}}, \quad (4)$$

$$\alpha = \frac{\bar{P}_C + \pi_I - P_I}{\pi_{EA}}, \quad (5)$$

$$\beta = \frac{\Delta P_C}{\pi_{EA}}, \tag{6}$$

$$B_1 = \frac{a_1 C_{EA}}{\pi_{EA}}, \tag{7}$$

$$B_2 = \frac{a_2 C_{EA}^2}{\pi_{EA}} = 1 - B_1, \tag{8}$$

where π_{EA} and Q_{EA} are efferent arteriolar oncotic pressure and efferent arteriolar plasma flow rate, respectively, $\bar{P}_C$ is the mean peritubular capillary hydrostatic pressure, and $\Delta P_C = P_C(0) - P_C(1)$ is the axial pressure drop along the capillary due to flow. The empirical constants a_1 and a_2 arise from an equation which gives oncotic pressure (π) as a quadratic function of C:

$$\pi = a_1 C + a_2 C^2. \tag{9}$$

For plasma protein concentrations in the range $4 \leq C \leq 10$ g/100 ml, $a_1 = 1.629$ mm Hg/(g/100 ml) and $a_2 = 0.2935$ mm Hg/(g/100 ml)^2. Substitution of the solution to Eq. 3 into Eq. 9 permits calculation of $\pi_C(x^*)$.

Eq. 3 assumes P_C to decline linearly with distance.

$$P_C = \bar{P}_C - \Delta P_C\,(x^* - \tfrac{1}{2}). \tag{10}$$

The actual decline in P_C due to flow is probably a nonlinear function of distance, especially since the flow rate changes nonlinearly as fluid is reabsorbed. As will be shown, however, the magnitude of ΔP_C usually has little effect on the computed value of APR, so that the functional form assumed for $P_C(x^*)$ likewise is not crucial as long as P_C decreases smoothly and monotonically.

For specified values of H, α, β, B_1, and B_2, solving Eq. 3 numerically yields the intracapillary protein concentration profile, including $C^*(1)$. The corresponding rate of reabsorption is then calculated from

$$\text{APR} = Q_{EA}\left[\frac{1}{C^*(1)} - 1\right]. \tag{11}$$

Conversely, given $C^*(1)$, α, β, B_1, and B_2, an iterative procedure (see Appendix) is used to find H and thus K_r, a quantity which cannot be evaluated directly from data.

GENERAL RESULTS

In this section the model is used to examine the effects on APR of variations in C_{EA} or Q_{EA}. Since P_I and π_I have yet to be directly measured, each of the following computations will be performed for several assumed values of the quantity $\pi_I - P_I$. An upper limit for P_I may be inferred by reasoning that it cannot greatly exceed intratubular pressures without causing tubule collapse. The lowest tubule pressures

(found in the distal tubule) are about 7 mm Hg (11), so that P_I probably does not exceed 10 mm Hg. The lower limit for π_I is clearly 0, so that the lower limit for the quantity $\pi_I - P_I$ is about -10 mm Hg. The upper limit for $\pi_I - P_I$ is set by the requirement that $P_r > 0$ at all points along the capillary. For the portion of the peritubular capillaries under consideration, $\pi_I - P_I$ must be less than approximately 20 mm Hg.

For the discussion in this section only, we have chosen for a reference state values of Q_{EA}, C_{EA}, $\bar{P}_C$, and APR representative of those measured in normal hydropenic rats (9–12), together with an intermediate value of ΔP_C. These quantities, given in the upper portion of Table I, are sufficient to calculate β, B_1, and B_2 from Eq. 6–8. For any assumed value of $\pi_I - P_I$, α may be found from Eq. 5.

In order to find H for the reference state it is necessary to compute a value for K_r which will yield APR = 20.0 nl/min (Table I) or equivalently, $C^*(1) = 80/(80 + 20) = 0.800$. K_r, like α, is a function of the value assumed for $\pi_I - P_I$: the larger the value of $\pi_I - P_I$, the smaller the net driving force, and the larger the K_r needed to give the required value of APR. The values for H and α corresponding to four assumed values of $\pi_I - P_I$ are given along with β, B_1, and B_2 in the lower portion of Table I.

Fig. 2 shows the profiles of π_C and $P_C + \pi_I - P_I$ computed by solving Eq. 3 for the parameters given in Table I. The numbering of the curves in this and subsequent figures corresponds to the four assumed values of $\pi_I - P_I$. The π_C curves for cases 1 and 2 differ only slightly and are shown as identical. The condition for exact equilibrium of the opposing pressures, $\Delta P = \Delta\pi$, is equivalent to $\pi_C = P_C + \pi_I - P_I$, so that case 4 ($\pi_I - P_I = 15.9$ mm Hg) can be seen to be nearest equilibrium

TABLE I

PHYSIOLOGICAL QUANTITIES AND MODEL PARAMETERS DEFINING THE REFERENCE STATE OF FIGS. 2, 3, AND 4

Physiological quantities:

C_{EA} = 9.0 g/100 ml	Q_{EA} = 80.0 nl/min
$\bar{P}_C$ = 7.2 mm Hg	APR = 20.0 nl/min
ΔP_C = 3.8 mm Hg	

Model parameters:

Case no.	$\pi_I - P_I$	α	H
	mm Hg		
1	−7.2	0.0	0.301
2	0.5	0.2	0.398
3	8.2	0.4	0.589
4	15.9	0.6	1.16

$B_1 = 0.381$, $B_2 = 0.619$, and $\beta = 0.100$ for all values of $\pi_I - P_I$.

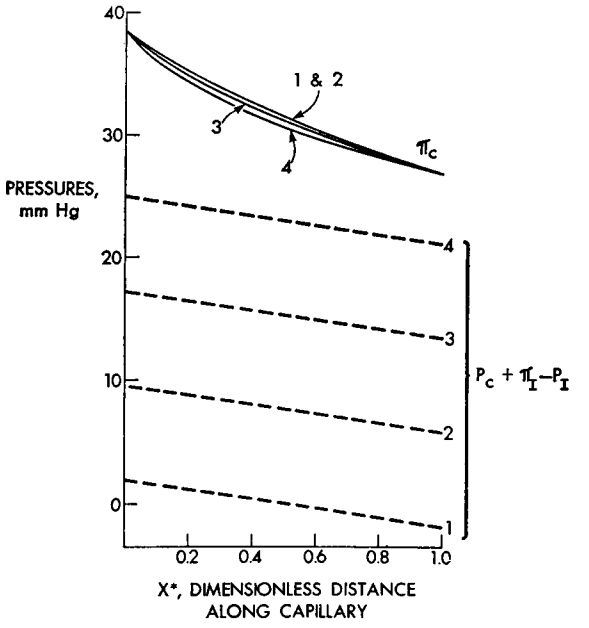

FIGURE 2 Peritubular transcapillary pressure profiles for the reference conditions given in Table I. Curves 1–4 correspond to the four values of $\pi_I - P_I$ in Table I.

and case 1 ($\pi_I - P_I = -7.2$ mm Hg) farthest away. Since both π_C and $P_C + \pi_I - P_I$ are declining continuously and since $d\Delta\pi/dx^* = 0$ when $\Delta P = \Delta\pi$, equilibrium can only be approached asymptotically. This is to be contrasted with the glomerulus, where the ΔP and $\Delta\pi$ curves may actually intersect (13).

To consider the effects on APR of variations in C_{EA} or Q_{EA}, let $\bar{P}_C + \pi_I - P_I$, ΔP_C, and K_r remain at their reference values. When Q_{EA} is varied with C_{EA} constant, H (according to Eq. 4) will vary inversely with Q_{EA} while α, β, B_1, and B_2 will be unchanged. When C_{EA} alone is altered, the variations in all five parameters must be calculated from the changes in C_{EA} and π_{EA}.

Fig. 3 shows the response of APR to variations in Q_{EA} ranging from roughly one-half to four times normal flow, with all other inputs remaining at their reference values. In each case the amount of reabsorption can be seen to increase with flow, but the rate of increase becomes less the higher the flow rate. As expected, the effect of flow is greatest when the driving pressures are closest to equilibrium, curve 4. For curves 1, 2, and 3, corresponding to pressures farther from equilibrium, the average effect of a fourfold increase in Q_{EA} (80 to 320 nl/min) is only about a 20% increase in reabsorption (20 to 24 nl/min). It should be noted, however, that all four curves show reabsorption to fall rapidly when Q_{EA} is reduced well below normal, an effect which may be very important in pathological states where renal perfusion is drastically reduced.

The effects of perturbations in C_{EA} are plotted in Fig. 4. Once again, the changes

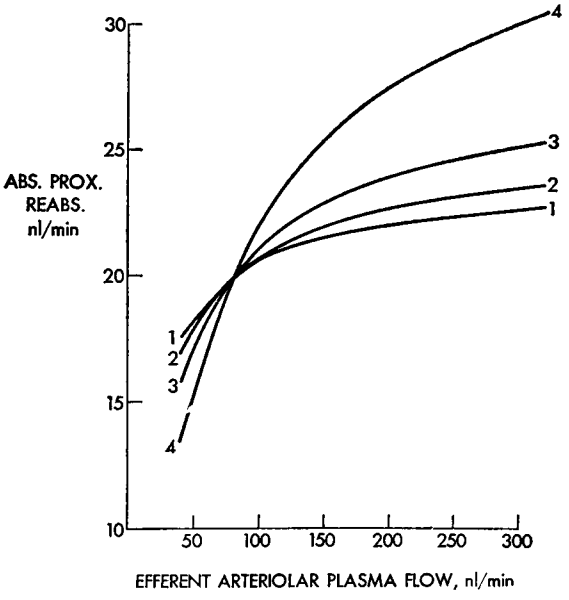

FIGURE 3

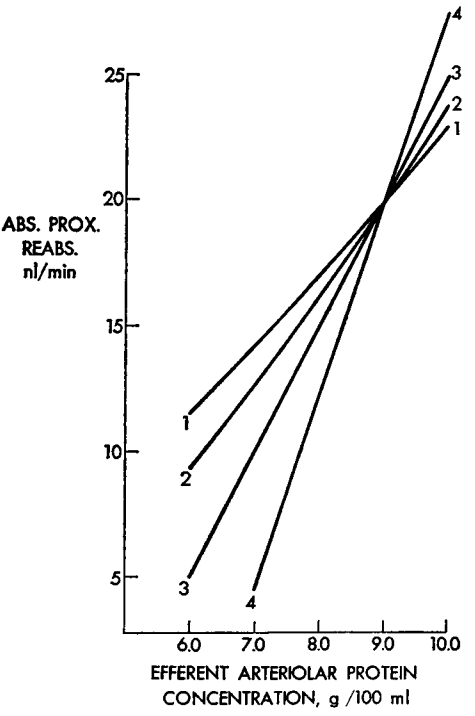

FIGURE 4

FIGURE 3 Absolute proximal reabsorption as a function of efferent arteriolar plasma flow. Curves 1–4 correspond to the four cases in Table I.

FIGURE 4 Absolute proximal reabsorption as a function of efferent arteriolar protein concentration. Curves 1–4 correspond to the four cases in Table I.

in reabsorption are most striking for pressures nearest equilibrium, but here the response of APR is almost linear in C_{EA}.

Comparison of Figs. 3 and 4 allows one to estimate the relative effects of changes in Q_{EA} and C_{EA}. Taking case 3 ($\pi_I - P_I = 8.2$ mm Hg) for example, Fig. 4 shows that a 1 g/100 ml (11%) increase in C_{EA} from its reference value of 9 g/100 ml would result in a 5 nl/min (25%) increase in APR. From Fig. 3 it can be seen that an increase in Q_{EA} from 80 to 280 nl/min (250%) would be required to bring about the same 25% increase in APR. It may be concluded from such comparisons that, while changes in reabsorption will parallel changes either in Q_{EA} or C_{EA} alone, the effect of C_{EA} is sufficient to predominate over opposing changes in Q_{EA} under most circumstances.

SPECIFIC APPLICATIONS OF THE MODEL

Only recently has it been possible to measure C_{EA}, Q_{EA}, $\bar{P}_C$, and APR, the quantities needed to allow application of the model to specific experimental conditions.

TABLE II

A SUMMARY OF SOME MEASURED DETERMINANTS OF PROXIMAL REABSORPTION IN THE RAT*

Study	C_{EA}	$\bar{P}_C$	Q_{EA}‡	APR
Brenner et al. (14)	*g/100 ml*	*mm Hg*	*nl/min*	
Plasma loading				
Preconstriction	8.3	10.2§	154	21.4
Aortic constriction	8.2	9.7§	114	19.2
Brenner and Troy (12)				
Normal hydropenia				
Preconstriction	9.1	7.2§	82.2	20.9
Aortic constriction	7.4	6.7§	85.7	13.9
Daugharty et al. (11)				
Normal hydropenia	9.0	6.4	88.6	22.5
Plasma loading	8.8	8.1	166	24.6
Normal hydropenia	8.6	5.5	74.0	20.2
Ringer loading	6.1	6.1	108	14.4

* All quantities reported are mean values.

‡ Computed from single nephron glomerular filtration rate (SNGFR) and filtration fraction (SNFF): Q_{EA} = SNGFR (1/SNFF − 1).

§ Obtained from another study in the same laboratory performed under similar conditions (9).

Results from studies (11, 12, 14) which provide this information for four different experimental maneuvers are summarized in Table II. Brenner et al. (14) constricted the abdominal aorta of rats which had been volume expanded with isoncotic plasma, thus lowering Q_{EA} with C_{EA} and $\bar{P}_C$ remaining essentially constant. Brenner and Troy (12) performed aortic constriction with normal hydropenia as control, and observed a large decline in C_{EA} but little change in either Q_{EA} or $\bar{P}_C$. Daugharty et al. (11), again using normal hydropenia as control, volume-expanded rats either with isoncotic plasma or isotonic Ringer's solution. Plasma loading brought about increases in Q_{EA} and $\bar{P}_C$, and a slight decline in mean C_{EA}. Ringer loading also increased Q_{EA} and $\bar{P}_C$, but brought about a large decline in C_{EA}. Thus, these studies allow application of the model to experimental data where Q_{EA}, C_{EA}, and $\bar{P}_C$ were changing either singly or in combination.

The procedure for applying the model to these studies is similar to that used to obtain Figs. 2–4. For a given maneuver, values of K_r for the control state were found for several assumed values of $\pi_I - P_I$. Then, assuming $\pi_I - P_I$ and K_r were unchanged by the maneuver and that ΔP_C remained in the 3–4 mm Hg range, new values for the model parameters were computed from the observed changes in the mean values of Q_{EA}, C_{EA}, and $\bar{P}_C$. Integrating Eq. 3 using the new parameters gave a "predicted" value of $C^*(1)$ for the maneuver. Finally, Eq. 11 was used to compute a value of APR for comparison to the experimental mean.

The study of Brenner et al. (14) involving aortic constriction in plasma-loaded

rats, offers the most direct experimental assessment of the isolated effect of a change in Q_{EA}. Table III shows values of APR calculated for $\pi_I - P_I$ ranging from −6.8 to 16.8 mm Hg and ΔP_C varying from 0 to 7.7 mm Hg. Comparison of the predicted and observed values of APR indicates that $\pi_I - P_I = 11$ mm Hg provides the best fit to the data. Based, however, upon a variation of 1 SE above or below the observed mean APR, the uncertainty in $\pi_I - P_I$ is large, the range of values being about 0–15 mm Hg.

Note in Table III that for all values of $\pi_I - P_I$ except the highest, APR calculated for different choices of ΔP_C varies by 2% or less. Efferent arteriolar hydrostatic pressure after plasma loading has been measured to be 14.5 mm Hg (11). Since renal vein pressure under these conditions has been measured to be roughly 5 mm Hg (11), $0 \leq \Delta P_C \leq 7.7$ covers essentially the entire possible range of axial pressure drops. Since calculations for other conditions show an insensitivity to ΔP_C similar to that reported in Table III, we have used only intermediate values of ΔP_C, 3–4 mm Hg, elsewhere in this paper.

The calculated and observed effects on APR of a large fall in C_{EA} (with little change in Q_{EA} or $\bar{P}_C$) are shown in Table IV. The 7 nl/min decline in APR after a 1.7 g/100 ml decrease in C_{EA} is very similar to the estimate one would obtain from curves 2 or 3 in Fig. 4. The best choice for $\pi_I - P_I$ based on these data is 4 mm Hg, with a range of 0–8 mm Hg (based on 1 SE).

Table V shows the results for plasma loading, in which the calculated increase in APR is minor for all values of $\pi_I - P_I$. The observed increase in APR was somewhat larger, but was not found to differ significantly from 0 (11). With such a small

TABLE III

CALCULATED AND OBSERVED VALUES OF ABSOLUTE PROXIMAL REABSORPTION BEFORE AND DURING AORTIC CONSTRICTION IN PLASMA-LOADED RATS

Calculated:				
$\pi_I - P_I$	Preconstriction	Aortic constriction		
	All ΔP_C	$\Delta P_C = 0$	$\Delta P_C = 3.8$	$\Delta P_C = 7.7$
mm Hg	*nl/min*		*nl/min*	
−6.8	21.4	20.3	20.3	20.3
−3.5	21.4	20.2	20.2	20.3
−0.1	21.4	20.1	20.1	20.1
3.3	21.4	19.9	19.9	20.0
6.7	21.4	19.7	19.7	19.8
10.0	21.4	19.3	19.4	19.5
13.4	21.4	18.6	18.8	19.0
16.8	21.4	16.6	17.5	18.0
Observed:				
(Reference 14)	21.4 ±1.1 SE		19.2 ±0.9	

TABLE IV

CALCULATED AND OBSERVED VALUES OF ABSOLUTE PROXIMAL REABSORPTION BEFORE AND DURING AORTIC CONSTRICTION IN NORMAL HYDROPENIC RATS

Calculated: $\pi_I - P_I$	Preconstriction	Aortic constriction
mm Hg	*nl/min*	
−7.2	20.9	16.2
0.6	20.9	14.9
8.5	20.9	12.7
16.3	20.9	8.0
Observed:		
(Reference 12)	20.9 ±1.4 SE	13.9 ±1.1

TABLE V

CALCULATED AND OBSERVED VALUES OF ABSOLUTE PROXIMAL REABSORPTION IN RATS BEFORE AND DURING VOLUME EXPANSION WITH ISONCOTIC PLASMA

Calculated: $\pi_I - P_I$	Normal hydropenia	Plasma loading
mm Hg	*nl/min*	
−6.4	22.5	22.6
1.3	22.5	22.7
9.0	22.5	22.7
16.7	22.5	23.1
Observed:		
(Reference 11)	22.5 ±1.1 SE	24.6 ±1.5

increase in APR, it is not possible to differentiate among the values of $\pi_I - P_I$, but these data do provide some insight into the relative effects of changes in C_{EA} and Q_{EA}. Assuming the values of C_{EA} and Q_{EA} to be true means, the 0.2 g/100 ml decrease in C_{EA} was enough to offset a doubling of Q_{EA}.

The model calculations for all of the studies considered thus far have assumed $\pi_I - P_I$ to be unchanged by the experimental maneuver. When this assumption is applied to Ringer loading, as shown under "Ringer loading, $\pi_I - P_I$ constant" in Table VI, a substantial decrease in APR is calculated. A fall in C_{EA} from 8.6 to 6.1 g/100 ml causes APR to decline despite a 50% increase in Q_{EA}, as would be expected from Figs. 3 and 4. Quantitative agreement with the observed change in APR for

TABLE VI

CALCULATED AND OBSERVED VALUES OF ABSOLUTE PROXIMAL REABSORPTION IN RATS BEFORE AND DURING VOLUME EXPANSION WITH RINGER'S SOLUTION

Calculated:					
Normal hydropenia		Ringer loading, $\pi_I - P_I$ constant		Ringer loading, $\pi_I - P_I$ 5 mm Hg less	
$\pi_I - P_I$	APR	$\pi_I - P_I$	APR	$\pi_I - P_I$	APR
(*mm Hg*)	(*nl/min*)	(*mm Hg*)	(*nl/min*)	(*mm Hg*)	(*nl/min*)
−5.5	20.2	−5.5	12.8	−10.5	16.0
1.6	20.2	1.6	10.7	−3.4	14.9
5.2	20.2	5.2	9.2	0.2	14.0
8.8	20.2	8.8	7.0	3.8	12.7
Observed:					
(Reference 11)	20.2 ±1.0 SE		14.4 ±1.4		14.4 ±1.4

constant $\pi_I - P_I$ is not, however, as good as for the maneuvers previously considered.

Ringer loading both expands plasma volume and (unlike plasma loading) decreases plasma oncotic pressure. It is not unlikely that this relatively large volume of hypooncotic plasma would result in net fluid loss to the interstitial space of the kidney. If this occurs, $\pi_I - P_I$ might be reduced by virtue of an increase in P_I (as when more fluid is forced into an elastic compartment) and a decrease in π_I (from dilution of interstitial colloids). This view is supported indirectly by the observation that the protein concentration in canine renal (hilar) lymph, thought to be similar to the interstitial concentration, declines during saline diuresis (21). The assumption of constant $\pi_I - P_I$ for Ringer loading may therefore be inappropriate. If we assume $\pi_I - P_I$ to decrease after loading by the arbitrary amount of 5 mm Hg, the calculated values of APR are as given in the right-hand column of Table VI, under the heading "Ringer loading, $\pi_I - P_I$ 5 mm Hg less." Good agreement with the observed APR was obtained for $\pi_I - P_I$ declining from 4 (control) to −1 mm Hg (loading).

DISCUSSION

Models dealing with fluid reabsorption in the renal proximal tubule have generally been constructed such that transport across the tubule, rather than the peritubular capillaries, governs the net rate of reabsorption. In their theoretical treatment of proximal reabsorption, Bossert and Schwartz (22) considered tubule distensibility to be the major factor governing reabsorption. Palatt et al. (23) treated the peritubular capillaries and the interstitial space essentially as a single compartment, thereby assuming again that transepithelial transport is rate limiting. Koushanpour

et al. (24) entirely neglected the peritubular capillary in their model of normal nephron function. Jacquez et al. (25) attempted a more comprehensive analysis, deriving equations for transport of several solutes and water not only across the epithelium at all levels of the nephron, but also across adjacent peritubular capillaries. Unfortunately, since solutions to their formidable set of coupled transport equations were not provided, no physiological conclusions about the control of reabsorption could be reached.

The present model is based on the assumption that the peritubular capillaries, not the tubules, exert primary control over the net rate of proximal reabsorption. As discussed elsewhere (12, 14), this concept is supported by a wealth of recent experimental evidence. With respect to the effects on net proximal reabsorption of changes in efferent arteriolar protein concentration and plasma flow rate, calculations based on the present model yield good qualitative and quantitative agreement with several recent micropuncture studies in the rat (11, 12, 14, 15).

A quantity needed as an input to the model but not directly available from experimental data is K_r, the reabsorption coefficient in Eq. 1. This coefficient was computed separately for each set of data by fitting the model result to the mean value of APR measured under control conditions. The validity of this approach can be tested by comparing the values of K_r calculated from different sets of data. If K_r truly characterizes the capillary network, values obtained for different groups of adult rats should be similar. This was indeed found to be the case. For example, assuming that $\pi_I - P_I = 5$ mm Hg and $\beta = 0$, K_r for the four studies listed in Table II varied little, ranging from 1.1 to 1.4 nl/(min·mm Hg) and averaging 1.2 nl/(min·mm Hg).

On the basis of our calculations using the data in Table II, the quantity $\pi_I - P_I$ appears to be in the range of 0–10 mm Hg, with 6 mm Hg providing a somewhat better fit to all of the data than other values. This result may be compared with values derived from indirect measurements of π_I and P_I. Using an implanted catheter technique, P_I has been found to be about 3 mm Hg (3.8 ± 2.0 cm H_2O) in the rat kidney (26). The protein concentration in renal (hilar) lymph is generally assumed to be similar to that in the cortical interstitium[8] and has been measured to be some 40% of the plasma level in the rat (Brenner and Troy, unpublished observations), sheep (27), and dog (21). If we assume the interstitial protein concentration in the rat kidney also to be some 40% of the normal plasma level of 6.0 g/100 ml, we obtain $\pi_I = 6$ mm Hg from the equation of Landis and Pappenheimer for plasma proteins (28). Therefore, from indirect experimental evidence, $\pi_I - P_I = 3$ mm Hg, a value in close agreement with the estimate of 6 mm Hg obtained using the model and the data in Table II.

[8] In support of this assumption, B. M. Brenner and J. L. Troy (unpublished observations) have recently found essentially identical protein concentrations in hilar lymph and in the fluid obtainable from the subcapsular (cortical) surface of the rat kidney. These paired measurements of protein concentration range from 2 to 3 g/100 ml in normal hydropenia.

There has not been general agreement in the experimental literature on the extent to which variations in peritubular capillary plasma flow rate alter the rate of reabsorption by the proximal tubule. Brenner and co-workers (11, 12, 14, 15) have generally found little flow dependence, while the findings of Lewy and Windhager (29), Daugharty et al. (30), and Schrier and Humphreys (31) indicate that, at least under certain conditions, variations in plasma flow may have significant effects on reabsorption. Fig. 3 suggests that these differing degrees of flow dependence might be explained by variations in the extent to which equilibrium is approached, that is, how closely $\Delta\pi$ approaches ΔP by the distal end of a capillary segment. In Fig. 3, curve 4 corresponds to pressures closest to equilibrium and shows the greatest flow dependence of reabsorption; curve 1 is farthest from equilibrium and shows the least flow dependence. While in the latter three studies (29–31) not all of the critical variables were measured, we can use evidence obtained by others (*vide infra*) under comparable conditions to suggest, in retrospect, that the experimental design of these studies may have favored a closer approach to equilibrium than is normally the case.

Lewy and Windhager (29) found absolute proximal reabsorption in the normal hydropenic rat to correlate closely with renal plasma flow during partial renal venous occlusion, when $\bar{P}_C$ was measured to be more than twice the normal control value, but found no such correlation during the control period. Since $\bar{P}_C$ has been shown in the rat to increase at about the same rate as venous pressure in response to progressive renal venous occlusion (32), and since indirect estimates of P_I under these conditions indicate that P_I rises much less rapidly than venous pressure (33), it may be inferred that ΔP also rises during partial renal venous occlusion. Although oncotic pressures were not measured, it is reasonable to suppose that ΔP more nearly equaled $\Delta\pi$ during partial venous constriction than during control, leading to a situation more like curve 4 in Fig. 3 and therefore to stronger flow dependence of reabsorption than in the normal control.

The results of Daugharty et al. (30), which show changes in proximal reabsorption after various maneuvers in the dog to be best correlated with changes in plasma flow, may also be reevaluated in terms of the expected degree of pressure equilibrium. In order to study changes in proximal reabsorption using clearance techniques, these authors employed the technique of diuretic blockade of distal tubule sodium reabsorption. Various strong diuretics, which increase intratubular flow rate, have been shown to increase markedly proximal tubule pressure (34–36), and $\bar{P}_C$ has been shown to parallel proximal tubule pressure under a variety of conditions that raise the latter (10, 32, 36, 37). Again, although postglomerular protein concentration was not measured, we may reasonably expect that with elevations in $\bar{P}_C$, ΔP would have approached $\Delta\pi$ more closely than normal, thereby again predisposing to an unusually strong degree of plasma-flow dependence of reabsorption. Finally, Schrier and Humphreys (31) observed changes in proximal reabsorption to be closely correlated with changes in renal plasma flow both in saline-loaded dogs and dogs undergoing water diuresis. Since these conditions also result in elevations in proximal

tubule hydrostatic pressure (38) and therefore in $\bar{P}_C$, as well as in hemodilution and consequent lowering of plasma protein concentration and $\bar{\pi}_C$, the experimental design again favored equilibrium. It should be pointed out that although decreases in $\pi_I - P_I$ may also have occurred, they would not be expected to compensate fully for the changes in $\bar{P}_C$ and $\bar{\pi}_C$.

Based on the foregoing, the seemingly contradictory findings regarding the extent of flow dependence of reabsorption observed on the one hand by Brenner and coworkers (11, 12, 14, 15) and on the other by Lewy and Windhager (29), Daugharty et al. (30), and Schrier and Humphreys (31) may now be explained very simply. In the former group of studies (11, 12, 14, 15), since the peritubular capillary hydrostatic and oncotic pressures were found to be at or near normal, the finding of little plasma-flow dependence of reabsorption suggests that ΔP and $\Delta\pi$ were far from equilibrium. In the latter studies (29–31), the evidence discussed makes it likely that ΔP and $\Delta\pi$ were close to equilibrium, thereby accounting for the greater degree of flow dependence observed under these conditions.

A very recent micropuncture study in the dog by Knox et al. (39) is particularly interesting in that, in contrast to the above studies in the dog (30, 31), the determinants of proximal reabsorption were measured under conditions which did not favor an abnormally close approach to equilibrium. Reabsorption was studied before and after infusion of hyperoncotic albumin solution, and all of the inputs needed for the model, including π_I (estimated from hilar lymph protein concentration) and P_I (estimated using an implanted capsule technique [33]), were either measured or can be calculated from the data given. After albumin infusion, C_{EA} declined from an average value of 8.1 to 7.8 g/100 ml, $\bar{P}_C$ remained constant at 15.5 mm Hg, and we estimate that $\pi_I - P_I$ increased from -1.8 to $+1.9$ mm Hg while Q_{EA} increased from 3.17 to 5.57 nl/s. Using these inputs and calculating K_f as before from the value of APR measured during control (0.52 nl/s), we compute that APR after albumin infusion should have fallen to 0.40 nl/s, almost identical with the measured value of 0.41 nl/s. Note that a modest fall in C_{EA} and a modest rise in $\pi_I - P_I$ were more than sufficient to offset the enhancing effect on reabsorption of a large increase in Q_{EA}. On the basis of these results and the more qualitative discussion of other studies in the dog (30, 31) given above, the present model of the control of proximal tubule fluid reabsorption appears to be applicable to the dog as well as to the rat.

In summary, a simple mathematical model of the renal peritubular capillaries has been developed and employed to examine the effects on net proximal fluid reabsorption of changes in efferent arteriolar plasma flow rate (Q_{EA}) and protein concentration (C_{EA}). In general, the model predicts that relatively small perturbations in C_{EA} should exert a greater influence on reabsorption than even large changes in Q_{EA}. Variations either in C_{EA} or Q_{EA} have their most pronounced effects on reabsorption when ΔP and $\Delta\pi$ are closest to equilibrium. These theoretical results have been found to be entirely in accord with recent experimental observations.

Dr. Brenner is a Medical Investigator of the Veterans Administration.

These studies were supported in part with funds from the U.S. Public Health Service (AM 13888), Veterans Administration (101/1073.1), and the Stanford University Research Development Fund.

Address requests for reprints to Dr. B. M. Brenner, Veterans Administration Hospital, 4150 Clement Street, San Francisco, California 94121.

Received for publication 5 October 1972.

REFERENCES

1. INTAGLIETTA, M., R. F. PAWULA, and W. R. TOMPKINS. 1970. *Microvasc. Res.* **2**:212.
2. INTAGLIETTA, M., D. R. RICHARDSON, and W. R. TOMPKINS. 1971. *Am. J. Physiol.* **221**:922.
3. LANDIS, E. M. 1930. *Am. J. Physiol.* **93**:355.
4. LEE, J. S., L. H. SMAJE, and B. W. ZWEIFACH. 1971. *Circ. Res.* **28**:358.
5. RICHARDSON, D. R., and B. W. ZWEIFACH. 1970. *Microvasc. Res.* **2**:474.
6. ZWEIFACH, B. W., and M. INTAGLIETTA. 1968. *Microvasc. Res.* **1**:83.
7. BRENNER, B. M., J. L. TROY, and T. M. DAUGHARTY. 1971. *J. Clin. Invest.* **50**:1776.
8. BRENNER, B. M., J. L. TROY, T. M. DAUGHARTY, W. M. DEEN, and C. R. ROBERTSON. 1972. *Am. J. Physiol.* **223**:1184.
9. ROBERTSON, C. R., W. M. DEEN, J. L. TROY, and B. M. BRENNER. 1972. *Am. J. Physiol.* **223**:1191.
10. BRENNER, B. M., J. L. TROY, and T. M. DAUGHARTY. 1972. *Am. J. Physiol.* **222**:246.
11. DAUGHARTY, T. M., I.F. UEKI, D. P. NICHOLAS, and B. M. BRENNER. 1972. *Am. J. Physiol.* **222**: 225.
12. BRENNER, B. M., and J. L. TROY. 1971. *J. Clin. Invest.* **50**:336.
13. DEEN, W. M., C. R. ROBERTSON, and B. M. BRENNER. 1972. *Am. J. Physiol.* **223**:1178.
14. BRENNER, B. M., J. L. TROY, T. M. DAUGHARTY, and R. M. MACINNES. 1973. *J. Clin. Invest.* **52**:190.
15. BRENNER, B. M., and T. M. DAUGHARTY. 1972. *In* Symposium on the Renal Handling of Sodium. H.Wirz and F. Spinelli, editors. S. Karger AG., Basel. 64.
16. MOREL, F., and Y. MURAYAMA. 1970. *Pfluegers Arch. Eur. J. Physiol.* **320**:1.
17. MAUDE, D. L. 1970. *Am. J. Physiol.* **218**:1590.
18. GIEBISCH, G., R. M. KLOSE, G. MALNIC, W. J. SULLIVAN, and E. E. WINDHAGER. 1964. *J. Gen. Physiol.* **47**:1175.
19. BOULPAEP, E. L. 1972. *Am. J. Physiol.* **222**:517.
20. KEDEM, O., and A. KATCHALSKY. 1958. *Biochim. Biophys. Acta.* **27**:229.
21. LEBRIE, S. J. 1968. *Am. J. Physiol.* **215**:116.
22. BOSSERT, W. H., and W. B. SCHWARTZ. 1967. *Am. J. Physiol.* **213**:793.
23. PALATT, P. J., G. M. SAIDEL, and M. MACKLIN. 1970. *J. Theor. Biol.* **29**:251.
24. KOUSHANPOUR, E., R. R. TARICA, and W. F. STEVENS. 1971. *J. Theor. Biol.* **31**:177.
25. JACQUEZ, J. A., B. CARNAHAN, and P. ABBRECHT. 1967. *Math. Biosci.* **1**:227.
26. WUNDERLICH, P., E. PERSSON, J. SCHNERMANN, H. ULFENDAHL, and M. WOLGAST. 1971. *Pfluegers Arch. Eur. J. Physiol.* **328**:307.
27. MCINTOSH, G. H., and B. MORRIS. 1971. *J. Physiol. (Lond.).* **214**:365.
28. LANDIS, E. M., and J. R. PAPPENHEMIER. 1963. *Handb. Physiol.* **2**:961.
29. LEWY, J. E., and E. E. WINDHAGER. 1968. *Am. J. Physiol.* **214**:943.
30. DAUGHARTY, T. M., S. M. ZWEIG, and L. E. EARLEY. 1971. *Am. J. Physiol.* **220**:2021.
31. SCHRIER, R. W., and M. H. HUMPHREYS. 1972. *Am. J. Physiol.* **222**:379.
32. GOTTSCHALK, C. W., and M. MYLLE. 1956. *Am. J. Physiol.* **185**:430.
33. OTT, C. E., L. G. NAVAR, and A. C. GUYTON. 1971. *Am. J. Physiol.* **221**:394.
34. KOCH, K. M., T. DUME, H. H. KRAUSE, and B. OCHWADT. 1967. *Pfluegers Arch. Eur. J. Physiol.* **295**:72.
35. KRAUSE, H. H., T. DUME, K. M. KOCH, and B. OCHWADT. 1967. *Pfluegers Arch. Eur. J. Physiol.* **295**:80.

36. GOTTSCHALK, C. W., and M. Mylle. 1957. *Am. J. Physiol.* **189**:323.
37. KNOX, F. G., L. R. WILLIS, J. W. STRANDHOY, and E. G. SCHNEIDER. 1972. *Kidney International.* **2**:11.
38. LEVY, M., and N. G. LEVINSKY. 1971. *Am. J. Physiol.* **220**:415.
39. KNOX, F. G., L. R. WILLIS, J. W. STRANDHOY, E. G. SCHNEIDER, L. G. NAVAR, and C. E. OTT. 1972. *Am. J. Physiol.* **223**:741.

APPENDIX

Derivation of Eq. 3

Consider a cylindrical tube with surface area S, length L, hydraulic permeability k, and volumetric flow rate $Q(x)$. A mass balance over a disk of thickness Δx requires that

$$Q(x + \Delta x) = Q(x) + \left(\frac{kS}{L}\right) \Delta x P_r , \qquad (A\ 1)$$

where P_r is the net driving force for reabsorption given in Eq. 2. Rearranging Eq. A 1 and dividing by Δx gives

$$\frac{Q(x + \Delta x) - Q(x)}{\Delta x} = \left(\frac{kS}{L}\right) P_r . \qquad (A\ 2)$$

Taking the limit $\Delta x \to 0$ in Eq. A 2 gives the differential equation for volumetric flow rate:

$$\frac{dQ}{dx} = \left(\frac{kS}{L}\right) P_r , \qquad Q(0) = Q_{EA} . \qquad (A\ 3)$$

Since the cylinder is assumed to be impermeable to protein, the mass flow rate of protein m is constant, and the volumetric flow rate and protein concentration (C) are related according to

$$Q = \frac{m}{C} , \qquad \frac{dQ}{dx} = -\frac{m}{C^2}\frac{dC}{dx} . \qquad (A\ 4)$$

Therefore,

$$\frac{dC}{dx} = -C^2 \left(\frac{kS}{mL}\right) P_r , \qquad C(0) = C_{EA} . \qquad (A\ 5)$$

Nondimensionalizing with L, C_{EA}, and π_{EA} then gives

$$\frac{dC^*}{dx^*} = -C^{*2} \left(\frac{kS\pi_{EA}}{Q_{EA}}\right) \frac{P_r}{\pi_{EA}} , \qquad C^*(0) = 1, \qquad (A\ 6)$$

where $C^* = C/C_{EA}$ and $x^* = x/L$. Note that $K_r = kS$. Substituting Eq. 2 into Eq. A 6, with π_C from Eq. 9 and P_C from Eq. 10, finally yields Eq. 3.

Procedure for Computing K_r

In computing K_r, advantage was taken of the fact that Eq. 3 could be solved analytically for $\beta = 0$. The analytical solution to be used in a given case depends on the values of α and $B_1^2 + 4\alpha B_2$.

For $\alpha = 0$:

$$Hx^* = -\left(\frac{2B_2C^* - B_1}{2B_1^2C^{*2}}\right) - \frac{B_2^2}{B_1^3}\ln\left(\frac{C^*}{B_1 + B_2C^*}\right) + I_1. \qquad (A\ 7)$$

Let

$$T = \frac{B_1}{2\alpha^2}\ln\left|\frac{C^{*2}}{\alpha - B_1C^* - B_2C^{*2}}\right| - \frac{1}{\alpha C^*}. \qquad (A\ 8)$$

For $\alpha \neq 0$, $B_1^2 + 4\alpha B_2 > 0$:

$$Hx^* = T + \left(\frac{B_1^2 + 2\alpha B_2}{2\alpha^2\sqrt{B_1^2 + 4\alpha B_2}}\right)\ln\left|\frac{\sqrt{B_1^2 + 4\alpha B_2} + B_1 + 2B_2C^*}{\sqrt{B_1^2 + 4\alpha B_2} - B_1 - 2B_2C^*}\right| + I_2. \qquad (A\ 9)$$

For $\alpha \neq 0$, $B_1^2 + 4\alpha B_2 = 0$:

$$Hx^* = T + \frac{B_1^2 + 2\alpha B_2}{\alpha^2(B_1 + 2B_2C^*)} + I_3. \qquad (A\ 10)$$

For $\alpha \neq 0$, $B_1^2 + 4\alpha B_2 < 0$:

$$Hx^* = T + \left(\frac{B_1^2 + 2\alpha B_2}{\alpha^2\sqrt{-B_1 - 4\alpha B_2}}\right)\arctan\left[\frac{-B_1 - 2B_2C^*}{\sqrt{-B_1^2 - 4\alpha B_2}}\right] + I_4. \qquad (A\ 11)$$

Given $C^*(1)$, α, B_1, and B_2, the integration constants (I_1, I_2, I_3, I_4) were evaluated from the initial condition, $C^*(0) = 1$, allowing H to be calculated for $\beta = 0$. *Reguli-falsi* iteration was used to find H for $\beta \neq 0$, the $\beta = 0$ value being employed as the initial estimate. K_r was then calculated from Eq. 4.